

FIGURE S1



FIGURE S2

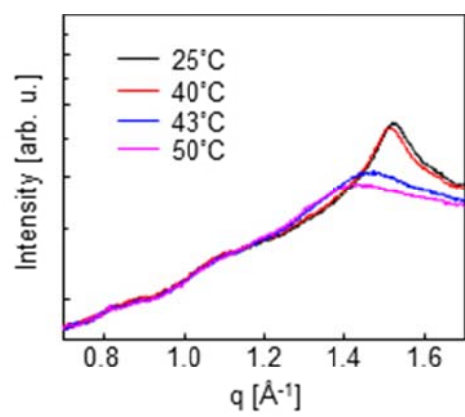


FIGURE S3

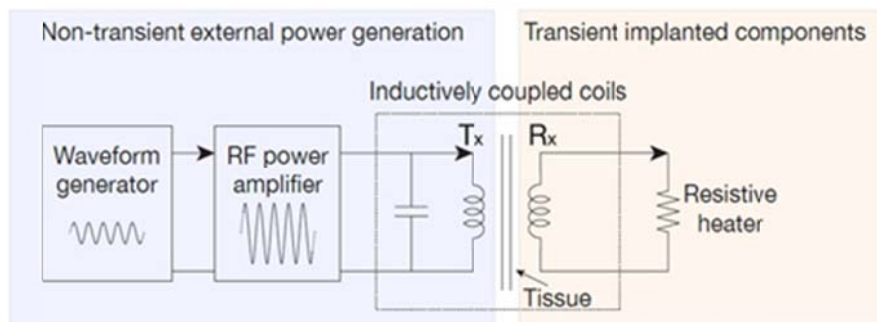


FIGURE S4

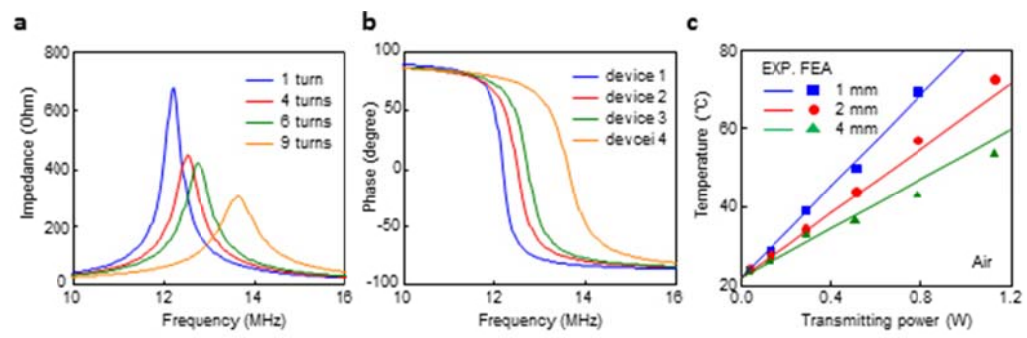


FIGURE S5

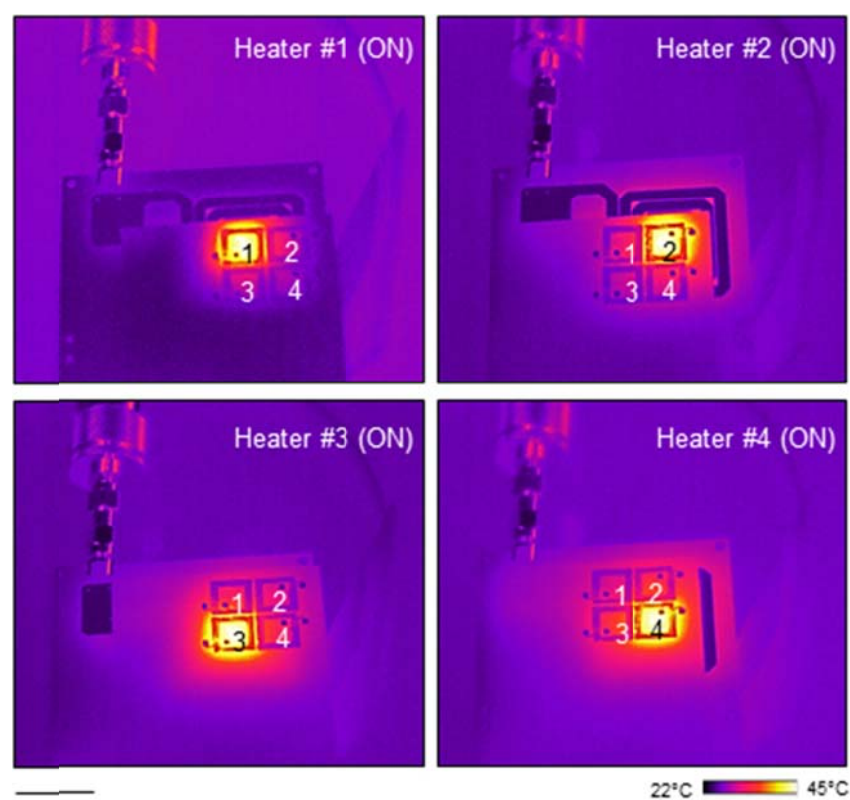


FIGURE S6

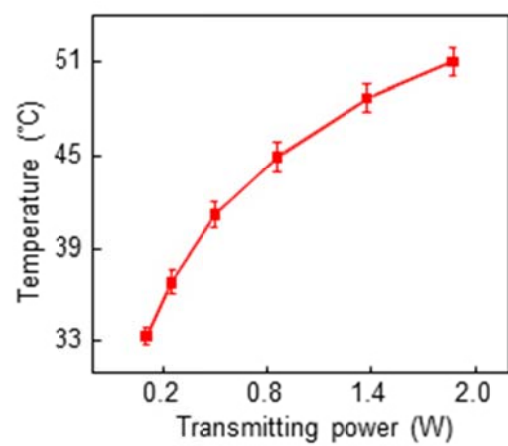


FIGURE S7

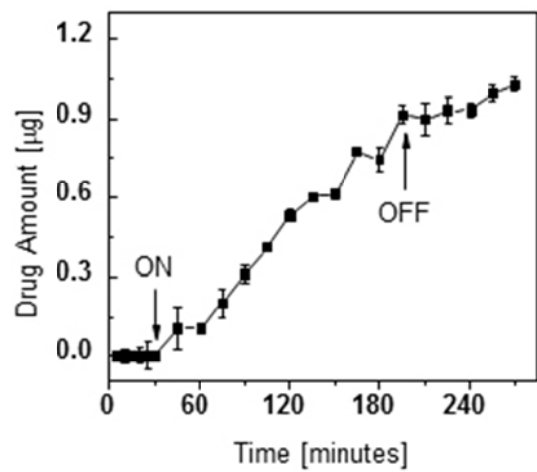


FIGURE S8

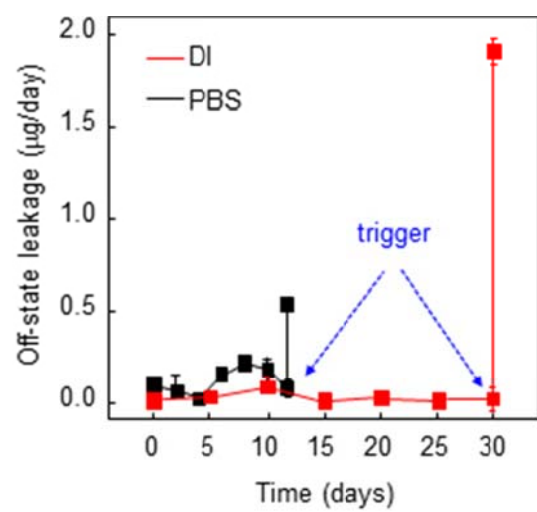


FIGURE S9

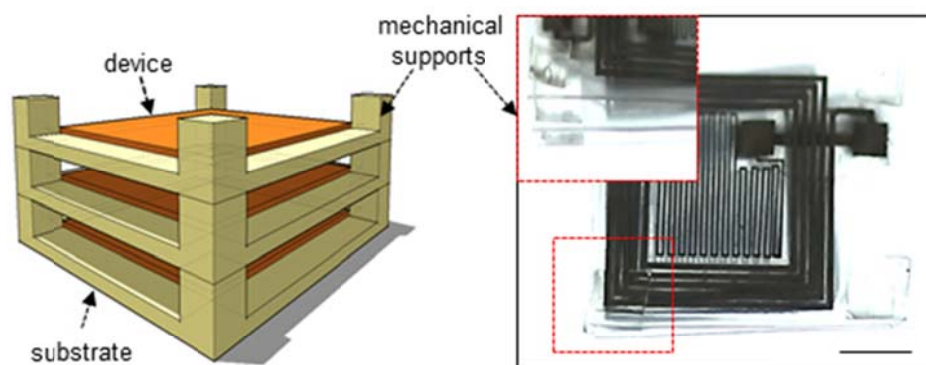


FIGURE S10

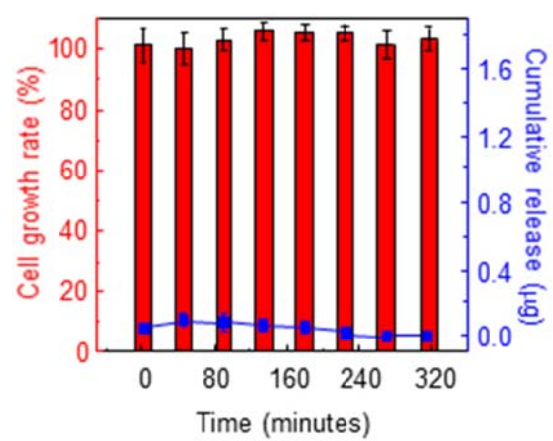


FIGURE S11

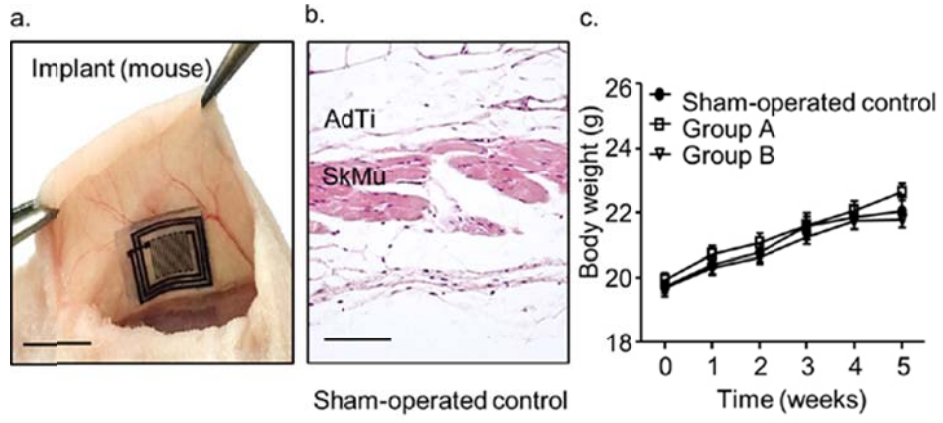


FIGURE S12

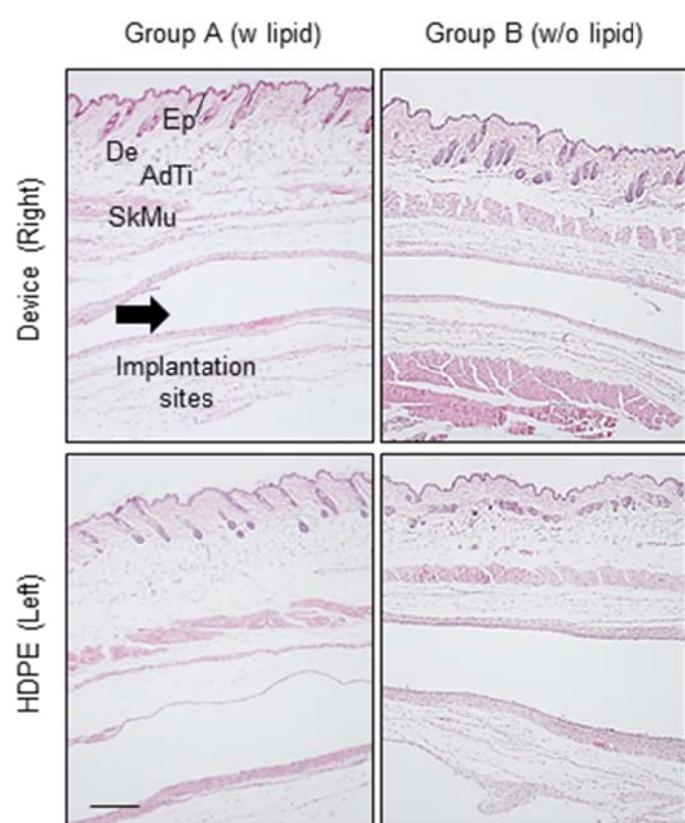


FIGURE S13

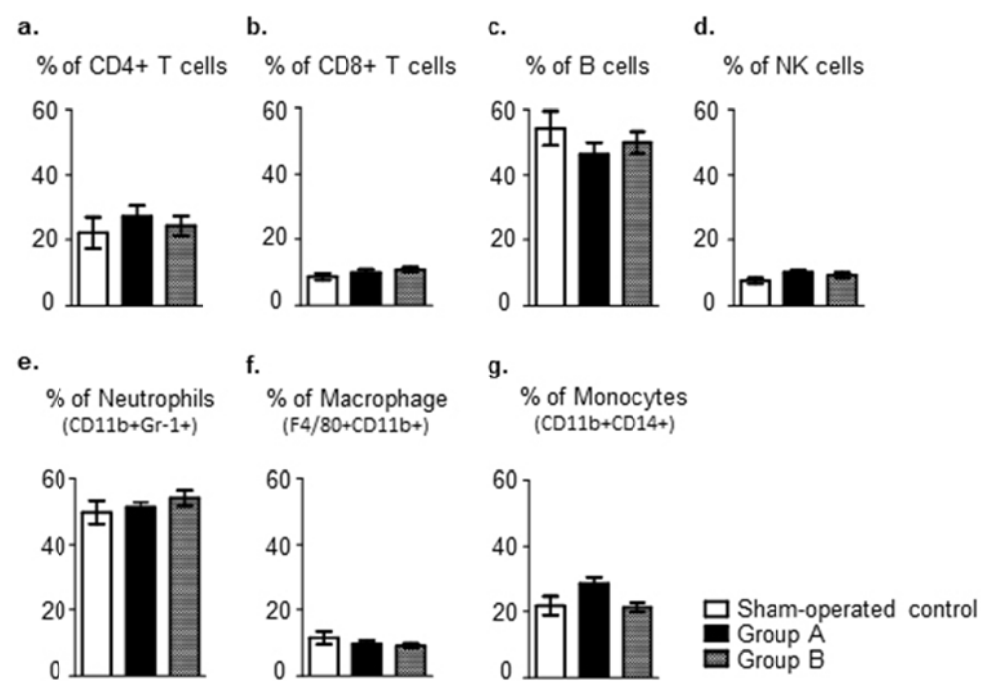


FIGURE S14

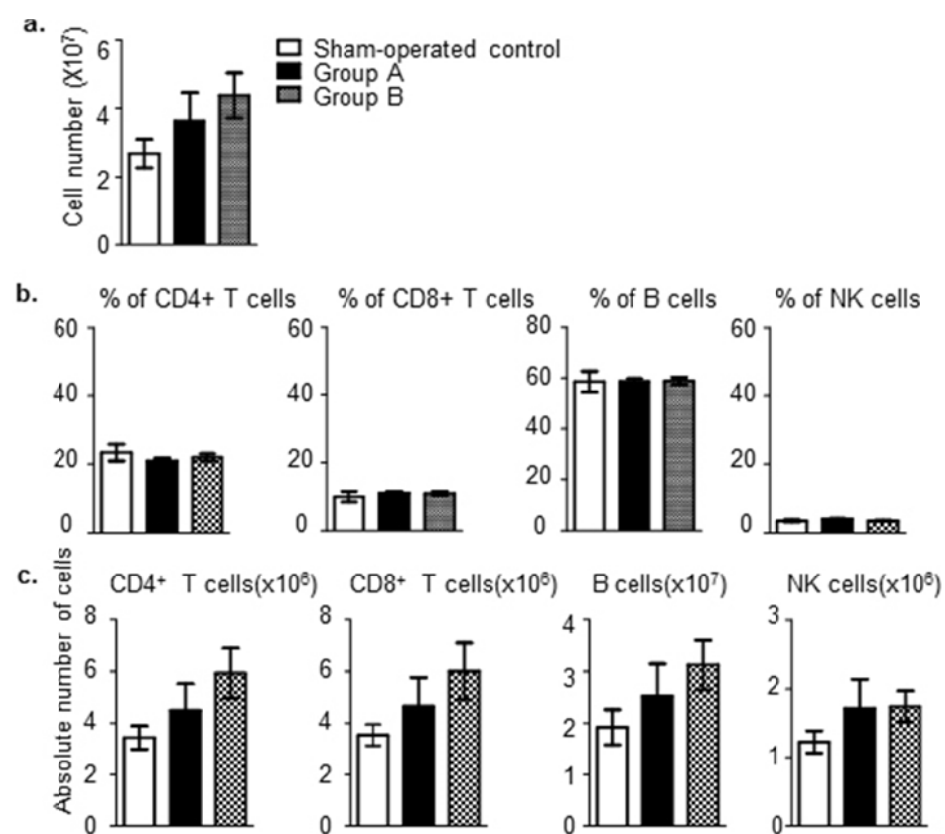


FIGURE S15

Implant	PMCs ^a	Lymphocytes ^b	Multinucleated giant cells ^c	Neovascularisation ^d	Fibrosis ^e
Sham-operation control	-	-	-	-	-
A HDPE	0.88 ± 0.34	0.88 ± 0.34	0.19 ± 0.4	0.75 ± 0.58	1.19 ± 0.4
sample	1.19 ± 0.4	0.63 ± 0.5	0.5 ± 0.52	0.75 ± 0.45	1.13 ± 0.5
B HDPE	0.42 ± 0.51	0.67 ± 0.65	0.58 ± 0.9	1 ± 0.74	1.58 ± 0.79
sample	0.81 ± 0.83	1.06 ± 0.44	0.44 ± 0.73	0.94 ± 0.57	1.25 ± 0.58

^a Polymorphonuclear cells: 1-5/phf* (1), 5-10/phf(2), >10/phf (3)

^b Lymphocytes: 1-5/phf (1), 5-10/phf(2), >10/phf (3), >10/phf (3)

^c Multinucleated giant cells: 1-5/phf (1), 5-10/phf(2), >10/phf (3)

^d Neovascularisation: Minimal capillary proliferation (1), Groups of 4-7 capillaries (2), Broad band of capillaries (3)

^e Fibrosis: Narrow band (1), Moderately thick band (2), Thick band (3)

* phf = per high powered (400 ×) field.

SI FIGURE LEGENDS

Figure S1 Standard curve for drug concentration calculation. Fluorescence intensity and drug concentration are linearly proportional from 0.001 g/ml to 1 g/ml for (a) dextran and (b) doxorubicin.

Figure S2 Two dimensional (2D) fluorescent optical images (scale bar: 500 μm) of lipid membrane (green), loaded drug (red) and their overlapped image (yellow).

Figure S3 Transmission Wide Angle X-ray Scattering (WAXS) scans of the lipid membrane at various temperatures.

Figure S4 Schematic diagram of the wireless power delivery system. A signal generator generates, amplifies, and delivers AC waveforms to a transmitter coil while an inductive coupling receiver coil receives these waveforms and delivers the power to a resistive heating element.

Figure S5 (a, b) Measured impedance and phase of the coupled transmitter and receiver for frequencies between 10 to 16 MHz. (c) Experimental (lines) and FEA (dots) results corresponding to changes in local temperature of an activating heater as a function of transmitter

driving power at different separations (1, 2, 4 mm) between the primary coil and the device, defined by the thickness of a piece of porcine tissue.

Figure S6 Collected infrared (IR) image (scale bar: 2 cm) during operation of all heating element in the 2×2 array device sequentially in a clockwise direction.

Figure S7 Doxorubicin release profile showing continued elution of drug (doxorubicin) after turned off the power early before the drug is completely released.

Figure S8 Changes in local temperature at the surface of an activated heater in phosphate buffer solution (PBS, 6 mL) as a function of transmitting power between 0.2 and 2.0 W.

Figure S9 Measured off-state leakage of doxorubicin from a lipid membrane laminated on a non-biodissolvable substrate (aluminium foil) over a month in deionized water (red line) and 12 days in PBS (black line).

Figure S10 Schematic illustration (left) and optical image (right) of a triple stacked device using mechanical supports made of PLGA. Inset (scale bar: 3 mm) shows an enlarge image at the edge.

Figure S11 Proliferation assay of the drug from the untriggered device and corresponding doxorubicin release profile showing leaked amount of drug has a negligible effect on cancer cell growth suppression. (n = 3, averaged data points and error bars are represented)

Figure S12 (a) Optical image (scale bar: 1cm) of subcutaneous implantation of a device into mice. (b) Histological examination (Scale bar: 100 μ m) of tissue sections in sham-operated control. Images of paraffin sections stained with Hematoxylin & eosin. SkMu; Skeletal muscle, AdTi; Adipose tissue. (c) Measurement of body weight of mice implanted with a device. Data are represented mean \pm SEM.

Figure S13 Histological examination (Scale bar: 100 μ m) of tissue sections in sham-operated control. Images of paraffin sections stained with Hematoxylin & eosin. SkMu; Skeletal muscle, AdTi; Adipose tissue.

Figure S14 **Immuno-profiling of lymphocytes from peripheral bloods at 5 weeks post-implantation of group A, B and operated-control groups.** (a) CD4⁺ T cells (CD3⁺CD4⁺), (b) CD8⁺ T cells (CD3⁺CD8⁺), (c) B cells (CD3⁺CD19⁺), (d) NK cells (CD3⁺NK1.1⁺), (e) Neutrophils (CD11b⁺Gr-1⁺), (f) Macrophage (F4/80⁺CD11b⁺), and (g) Monocytes (CD11b⁺CD14⁺) population are presented as percentages of total PBMCs in the peripheral blood by flow cytometry. (n = 10, mean \pm SEM)

Figure S15 Flow cytometric analysis of splenocytes from mice implanted with group A, B devices and sham-operated control at 5 weeks post-implantation. (a) Total number of splenocytes following sham-operated and two test groups. (b) Percentage of indicated cell populations using flow cytometry. (c) Absolute number of various immune cell subsets in spleen. Data presented are the means \pm SEM.

Table S1 Histological quantitative analysis of biocompatibility at five weeks post-implantation of group A and B materials. Randomly selected three fields per slide were counted at $\times 400$ magnification. Inflammatory cells (polymorphonuclear cells, lymphocytes, and multinucleated giant cells) infiltration were scored as described. Values are given as means \pm SEM.